The Hypothalamic Arcuate Nucleus–Median Eminence Is a Target for Sustained Diabetes Remission Induced by Fibroblast Growth Factor 1

Jenny M. Brown,[1] Jarrad M. Scarlett,[1,2] Miles E. Matsen,[1] Hong T. Nguyen,[1] Anna Secher,[3] Rasmus Jorgensen,[3] Gregory J. Morton,[1] and Michael W. Schwartz[1]

Diabetes 2019;68:1054–1061 | https://doi.org/10.2337/db19-0025

In rodent models of type 2 diabetes (T2D), sustained remission of diabetic hyperglycemia can be induced by a single intracerebroventricular (icv) injection of fibroblast growth factor 1 (FGF1). To identify the brain areas responsible for this effect, we first used immunohistochemistry to map the hypothalamic distribution of phosphorylated extracellular signal–related kinase 1/2 (pERK1/2), a marker of mitogen-activated protein kinase–ERK signal transduction downstream of FGF receptor activation. Twenty minutes after icv FGF1 injection in adult male Wistar rats, pERK1/2 staining was detected primarily in two hypothalamic areas: the arcuate nucleus–median eminence (ARC-ME) and the paraventricular nucleus (PVN). To determine whether an action of FGF1 localized to either the ARC-ME or the PVN is capable of mimicking the sustained antidiabetic effect elicited by icv FGF1, we microinjected either saline vehicle or a low dose of FGF1 (0.3 μg/side) bilaterally into either the ARC-ME area or PVN of Zucker Diabetic Fatty rats, a model of T2D, and monitored daily food intake, body weight, and blood glucose levels over a 3-week period. Whereas bilateral intra-arcuate microinjection of saline vehicle was without effect, remission of hyperglycemia lasting >3 weeks was observed following bilateral microinjection of FGF1 into the ARC-ME. This antidiabetic effect cannot be attributed to leakage of FGF1 into cerebrospinal fluid and subsequent action on other brain areas, since icv injection of the same total dose was without effect. Combined with our finding that bilateral microinjection of the same dose of FGF1 into the PVN was without effect on glycemia or other parameters, we conclude that the ARC-ME area (but not the PVN) is a target for sustained remission of diabetic hyperglycemia induced by FGF1.

Several members of the fibroblast growth factor (FGF) family of peptides have been shown to have antidiabetic properties when administered either systemically or centrally in rodent models of type 2 diabetes (T2D). Among these are the two "endocrine FGFs"—FGF19 and FGF21—and the tissue growth factor FGF1 (1–4). The centrally mediated antidiabetic effect of FGF1 is unique in that it lasts for weeks or months following a single intracerebroventricular (icv) injection in both mouse (*ob/ob* and *db/db*) and rat (Zucker Diabetic Fatty [ZDF]) models of T2D (3,5).

To better understand how FGF1 elicits this effect, we sought in the current work to identify the brain areas involved. To this end, we first mapped the central nervous system distribution of phosphorylated extracellular signal–related kinase 1/2 (pERK1/2), a cellular marker of FGF receptor activation, following icv injection FGF1 in normal rats. This work revealed robust FGF1-induced pERK1/2 staining in only two brain areas, both of which are known to express FGF receptors and implicated in glucose homeostasis: the hypothalamic arcuate nucleus–median eminence (ARC-ME) and the paraventricular nucleus (PVN) (6–8). To determine whether an action of FGF1 limited to either area is sufficient to recapitulate the sustained antidiabetic effect of FGF1 following icv administration, we microinjected into either the ARC-ME or PVN either saline vehicle or a dose of FGF1 fivefold below what is needed for efficacy following icv injection in separate cohorts of ZDF rats and monitored daily levels of food intake, body weight, and blood glucose for 3 weeks. We report that whereas sustained remission of hyperglycemia is elicited by FGF1 microinjection into the ARC-ME,

[1]Department of Medicine, UW Medicine Diabetes Institute, University of Washington, Seattle, WA
[2]Department of Pediatric Gastroenterology and Hepatology, University of Washington, Seattle, WA
[3]Diabetes Research, Global Drug Discovery, Novo Nordisk, Måløv, Denmark
Corresponding author: Michael W. Schwartz, mschwart@u.washington.edu

Received 8 January 2019 and accepted 14 February 2019

microinjection of the same low dose of FGF1 into the PVN of ZDF rats was without effect, despite robustly inducing pERK1/2 in this brain area. Moreover, the pERK1/2 immunoreactivity observed in the ARC-ME following icv FGF1 is concentrated in glial cells (tanycytes and astrocytes) rather than neurons, raising the possibility that neuronal responses to FGF1 are secondary to its action on glial cells. These findings collectively identify the ARC-ME as a key target for the sustained antidiabetic effect of FGF1.

RESEARCH DESIGN AND METHODS

Animals

All procedures were performed according to the National Institutes of Health Guide for the Care and Use of Laboratory Animals and approved by the Institutional Animal Care and Use Committee at the University of Washington. Animals were individually housed under specific pathogen-free conditions in a temperature-controlled room with a 12:12-h light/dark cycle and provided with ad libitum access to water and standard chow unless otherwise stated. Male, 6-week-old ZDF rats (ZDF-Leprfa/Crl) were purchased from Charles River Laboratories (Wilmington, MA) and provided ad libitum access to Purina 5008 chow (Animal Specialties, Inc., Hubbard, OR). Studies were performed on 8-week-old rats when blood glucose levels obtained under ad libitum–fed conditions are typically >250 mg/dL (9). For each study, groups receiving icv vehicle or FGF1 injection were matched for body weight and blood glucose levels. Male, 8-week-old Wistar rats were purchased from Harlan Laboratories (Madison, WI) to assess immunofluorescent pERK1/2 activation in the hypothalamus after icv FGF1 injection.

Intraparenchymal and Lateral Ventricle Guide Cannula Implantation

Rats were placed in a stereotaxic frame (Koph 1900; Cartesian Research Inc., Sandy, OR) and underwent surgical implantation of an indwelling bilateral cannula directed to the ARC or PVN (Plastics One, Roanoke, VA) under isoflurane anesthesia using stereotaxic coordinates: for ARC, −2.8 mm posterior to bregma, 0.5 mm lateral, and 8 mm depth; and for PVN, −1.8 mm posterior to bregma ± 0.5 mm lateral and 6.0 mm posterior to bregma below the skull surface. The cannula was secured to the skull with stainless steel screws and dental cement. To confirm cannula targeting, we microinjected Cy3-labeled FGF1 into the ARC-ME or PVN and assessed the distribution of the Cy3 label postmortem. In other animals, a single cannula was implanted in the lateral ventricle (LV) for icv injection as previously described (5). Animals were allowed to recover for at least 7 days before being studied.

Intraparenchymal and icv Injections

Rats were anesthetized under isoflurane anesthesia and placed in a stereotaxic device. Bilateral intraparenchymal injections of either saline vehicle or recombinant rat FGF1 (ProSpec-Tany TechnoGene Ltd., East Brunswick, NJ) dissolved in sterile water at a concentration of 1 μg/μL were microinjected over 3 min in a volume of 300 nL bilaterally (total dose 0.6 μg) using a Hamilton syringe (80030) with a 33-gauge needle that projected 1.5 mm beyond the tip of the cannula, at a rate of 75 nL/min (Micro4 controller; World Precision Instruments, Sarasota, FL), followed by a 5-min delay before needle withdrawal. The icv injection of either saline or FGF1 was performed at 1 week after cannulation of the LV. Injections were given over 1 min using a 33-gauge needle extending 2 mm beyond the tip of the LV cannula, as previously described (5).

Immunofluorescence

To detect FGF1-responsive brain areas, pERK1/2 (which reflects activation of the mitogen-activated protein kinase [MAPK]/ERK pathway) was detected by immunohistochemistry in habituated overnight-fasted Wistar rats. Twenty minutes following icv injection of either vehicle or recombinant FGF1 (3 μg), rats were anesthetized with ketamine and xylazine and perfused with PBS followed by 4% paraformaldehyde in 0.1 mol/L PBS, after which brains were removed. Anatomically matched free-floating coronal sections (35-μm thickness) were collected from −1.2 mm bregma to −14.7 mm bregma, washed in PBS at room temperature, permeabilized in Nonidet P-40 1% and 1.0% BSA for 10 min, blocked in freshly prepared 5% normal goat serum (Jackson ImmunoResearch Laboratories, West Grove, PA), and incubated overnight at 4°C with rabbit anti-pERK1/2 antibody (1:1,000) (#4370S; Cell Signaling Technology, Danvers, MA). To detect pERK (a marker of FGF receptor activation [10,11]) in tanycytes, neurons, or astrocytes, sections were incubated with chicken anti-vimentin (1:1,000) (ab24525; Abcam, Eugene, OR), mouse anti-NeuN (1:1,000) (MAB377; MilliporeSigma, Burlington, MA), or mouse GFAP-cy3 (1:1,000) (C9205; Millipore Sigma), respectively. After incubation at 4°C for 6 h with goat anti-rabbit Alexa Fluor 488 (secondary antibody) diluted 1:1,000, sections were washed overnight in PBS and mounted on slides. pERK1/2 immunofluorescence density was assessed in a semiquantitative manner as follows: ******/***** denotes a strong signal that occupies the entire region/nucleus, ****/*** is a moderate signal that occupies most of the region, and **/* denotes minimal signal occupying a small region (see Table 1). Immunofluorescence images were captured using a Leica SP8X Scanning Confocal microscope (Leica Microsystems, Buffalo Grove, IL) with an HC FLUOTAR L 25×/0.95 W objective.

Statistical Analysis

All results are expressed as mean ± SEM, and statistical comparisons were performed using R (12) with the interface RStudio (13). Longitudinal data were analyzed using a linear mixed model including fixed effect of treatment and day and random effects of animal. Linear mixed models were conducted with the R statistical package "nlme"

(14), one-way ANOVA, or the equivalent nonparametric test using the R statistical package "nparLD" (15). *P* values of <0.05 were considered significant.

RESULTS

icv FGF1 Injection Activates pERK1/2 Signaling in the ARC-ME and PVN

As a first step to identify candidate brain regions involved in the antidiabetic action of FGF1, we assessed the regional distribution of pERK1/2 immunoreactivity in serial coronal sections collected from optic chiasm to hindbrain in normal Wistar rats 20 min after icv injection of either FGF1 (3 μg) or saline vehicle. pERK1/2 immunoreactivity was detected primarily in the PVN and along the ventral surface of the third ventricle, extending into the parenchyma of the ARC-ME along its entire rostrocaudal axis (Table 1 and Fig. 1). These findings are consistent with the known distribution of FGF receptors in ARC-ME and PVN (7), and they identify these hypothalamic areas as potential targets for sustained remission of diabetic hyperglycemia induced by centrally administered FGF1. Although pERK signal intensity was also high in the supraoptic and suprachiasmatic nuclei, this was true for both vehicle- and FGF1-treated animals. Thus, these two brain areas do not stand out as being FGF1 responsive, although we cannot exclude the possibility that the high basal pERK precluded our ability to detect a response.

Effect of Intra–ARC-ME FGF1 Microinjection in ZDF Rats

Based on evidence that the minimum icv dose of FGF1 to induce sustained glucose lowering is 3.0 μg (refs. 3,5 and J.M.S., unpublished observations), we asked whether this effect can be recapitulated by delivery of a much lower dose directly into the ARC-ME of ZDF rats. A dual-guide cannula (Fig. 2*A*) was used to microinject into this brain area

Table 1—Distribution of pERK1/2 immunofluorescence in the rat brain after icv FGF1

			Treatment	
Brain region	Nucleus	Abbreviation	icv vehicle	icv FGF1
Hypothalamus	Suprachiasmatic	SCN	***	***
	Preoptic area	POA	*	*
	Supraoptic	SON	*****	******
	Paraventricular	PVN	***	*****
	Retrochiasmatic area	Rch	*	***
	Ventromedial hypothalamic n.	VMN	*	*
	Dorsomedial hypothalamic n.	DMN	*	**
	Arcuate hypothalamic n.	ARC	**	******
	Mammillary n.	MM	–	–
	Median eminence	ME	***	******
	Infundibular stalk	InfS	**	******
Thalamus	Paraventricular thalamic n. anterior	PVA	–	–
	Anteroventral thalamic n.	AV	–	*
	Anteroventral medial n.	AM	–	–
	Paratenial n.	PT	–	–
	Mediodorsal n.	MD	–	–
	Paraventricular thalamic n.	PV	–	–
	Paraventricular thalamic n. posterior	PVP	–	–
	Centromedial thalamic n.	CM	–	–
	Reuniens n.	Re	–	–
Amygdala	Medial amygdaloid n.	MeA	–	–
	Cortical amygdaloid n.	CoA	–	–
	Basolateral amygdaloid n.	BLA	–	–
	Basomedial amygdaloid n.	BMA	–	–
	Central amygdaloid n.	CeA	*	–
	Amygdalostriatal transition	Ast	–	–
Hippocampus	CA1 of the Ammon's horn	CA1	–	*
	CA2 of the Ammon's horn	CA2	–	–
	CA3 of the Ammon's horn	CA3	–	–
	Dentate gyrus	DG	–	*
Hindbrain	Raphe pallidus n.	Rpa	**	**
	n. of the solitary tract	NTS	–	–
	Area postrema	AP	–	**
	Hypoglossal n.	12N	*	*
	Spinal n. of trigeminal nerve	sp5	**	**

Positive signal density in an area or nucleus defined by a strong signal and a signal that occupies the entire region (******/*****), moderate signal and it occupies most of the region (****/***), little signal and it occupies a small region of the nucleus (**/*), and (–) no signal. CA, Cornu Ammonis; n., nucleus.

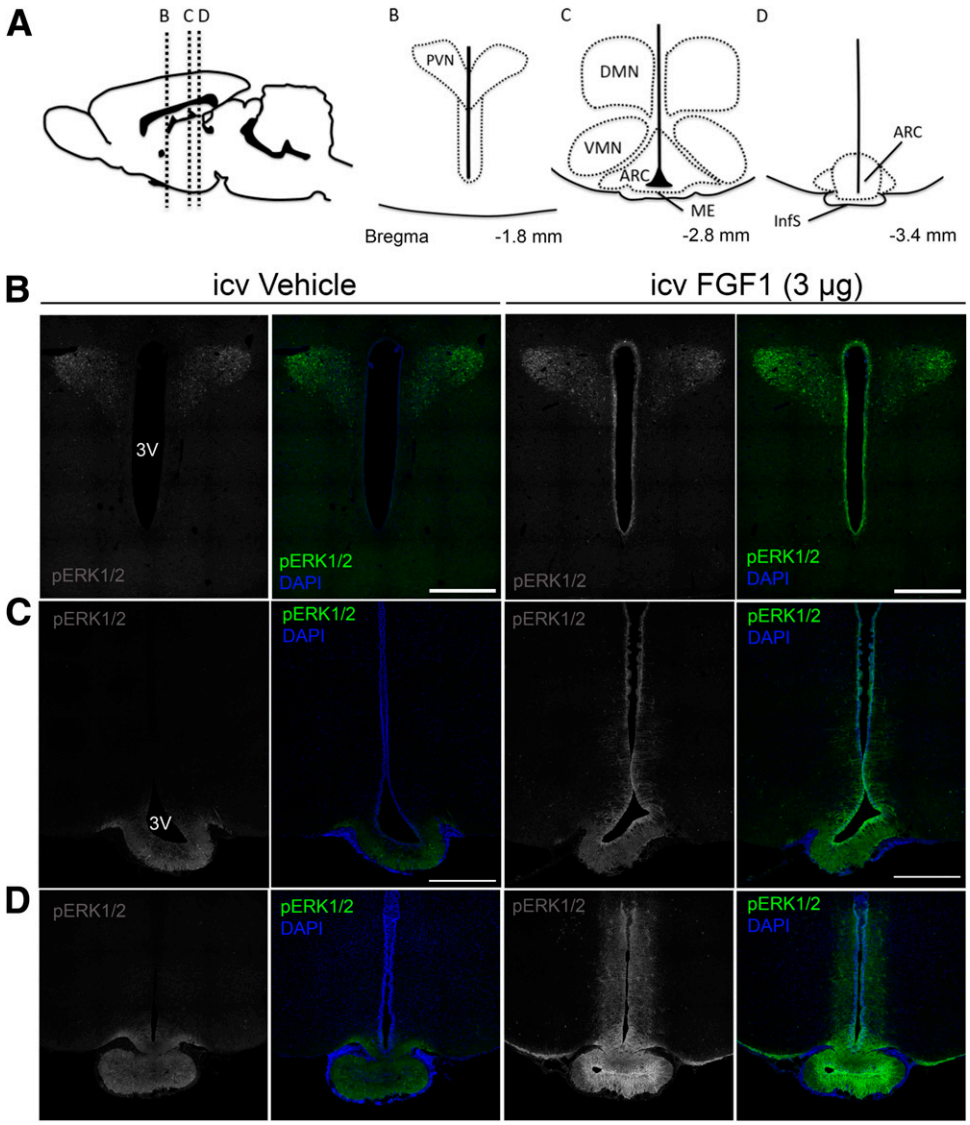

Figure 1—Regional activation of MAPK/ERK1/2 signaling in the hypothalamus after icv FGF1. *A*: Diagram at top shows sagittal view of the rat brain (left) and inserts of the mediobasal hypothalamus (right) showing orientation of panel images of the PVN, ARC, ME, ventromedial nucleus (VMN), dorsomedial nucleus (DMN), and infundibular stalk (InfS). *B–D*: Confocal images of coronal sections showing pERK1/2 (green) and DAPI (blue) obtained 20 min after icv injection of either vehicle or FGF1 (3 μg). Images are taken from the PVN (*B*), the ARC-ME (*C*), and InfS (*D*). Scale bars: 500 μm (*B* and *C*). 3V, third ventricle.

either vehicle or a dose of FGF1 fivefold below that necessary for efficacy when given icv (0.3 μg/side given bilaterally). We report that this intervention induced reductions of body weight and food intake (Fig. 2*C* and *D*) comparable to what is observed following the higher dose of FGF1 given icv (5). Moreover, mean blood glucose levels fell by ~50% (from 300 ± 22 to 158 ± 12 mg/dL; $P < 0.05$), whereas no effect was observed in vehicle-injected ZDF controls (Fig. 2*B*). This glucose-lowering effect was apparent within 48 h after intra–ARC-ME injection and persisted for ~3 weeks, mimicking the effect of higher-dose icv injection. In contrast, the same low dose of FGF1 (0.3 μg/side) did not reduce levels of blood glucose (Fig. 2*E*), food intake, or body weight (data not shown) following icv injection (Fig. 2*E*).

Having established that FGF1 action limited to the ARC-ME is sufficient to elicit sustained normalization of glycemia in ZDF rats (at a dose below that needed for efficacy when given icv), we sought to identify the cellular elements involved in this response. To this end, we used confocal microscopy to colocalize pERK1/2 with glial and neuronal markers in the ARC-ME of Wistar rats 20 min after icv injection of either FGF1 or vehicle. Given the prominent pERK1/2 activation induced by icv FGF1 in cells lining the third ventricle, we anticipated many of these cells would be tanycytes, and this was confirmed by our finding of extensive colocalization of pERK1/2 and vimentin immunostaining (Fig. 2*F* and *G*). Although we also observed colocalization of pERK1/2 with GFAP (+) astrocytes, colocalization with the neuronal marker NeuN was not observed (Fig. 2*I*).

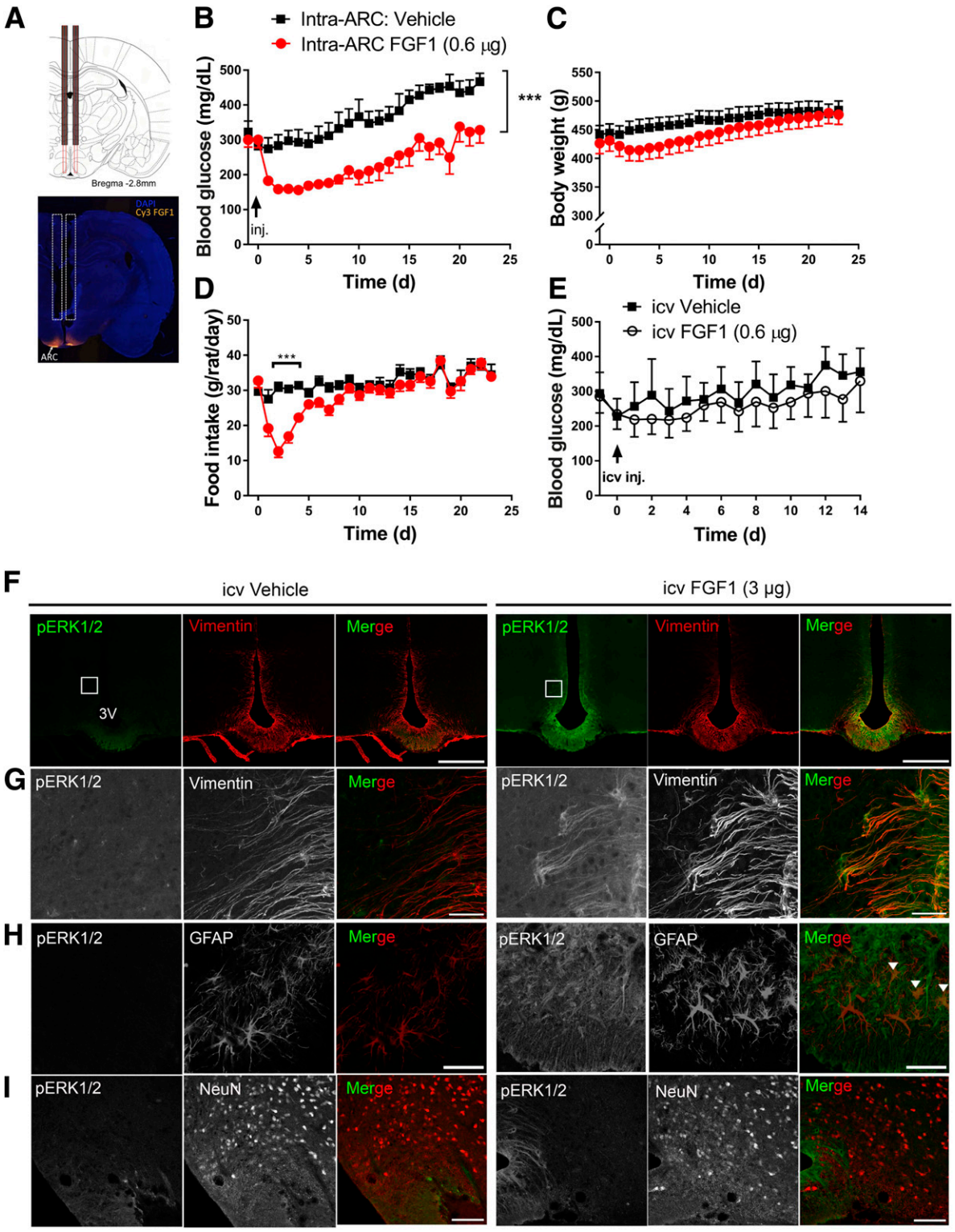

Figure 2—Effect of intra-ARC microinjection of FGF1 in ZDF rats. *A*: Scale diagram of bilateral intra-ARC guide cannula (top panel) and representative image of Cy3-labled FGF1 injectate spread following microinjection into the ARC area (bottom panel). Daily blood glucose (*B*), body weight (*C*), and food intake (*D*) from ZDF rats after a single bilateral intra-ARC microinjection of either vehicle ($n = 7$) (black squares) or FGF1 (0.3 μg/side, for a total of 0.6 μg; $n = 8$) (red circles). *E*: Daily blood glucose levels in ZDF rats after a single icv injection of either vehicle ($n = 4$) or FGF1 at a dose equal to that given by microinjection into the ARC (0.6 μg; $n = 4$). Significance determined by linear mixed-model analysis. Confocal images of coronal sections of the ARC-ME costained with antibodies to pERK1/2 (green) and markers of tanycytes (vimentin), astrocytes (GFAP), or neurons (NeuN) 20 min after icv injection of either vehicle (left panels, *F–I*) or FGF1 (3 μg) (right panels, *F–I*) in Wistar rats ($n = 5$/group). *G*: Higher magnification view of images shown in inset in *F*. Scale bars: 500 μm (*F*), 50 μm (*G* and *H*), 100 μm (*I*). Colocalization of GFAP and pERK1/2 denoted by white arrowheads in (*H*). Data are mean ± SEM. $^{***}P < 0.001$ vs. intra-ARC vehicle. 3V, third ventricle; d, days; inj., injection.

Effect of FGF1 Microinjection Into the PVN

We next sought to determine if the same low dose of FGF1 (0.6 μg) elicits sustained glucose lowering following microinjection into the PVN, rather than the ARC-ME, of ZDF rats (Fig. 3*A*). Unlike the potent effects on food intake, body weight, and blood glucose levels observed following FGF1 microinjection into the ARC area, microinjection into the PVN was without effect on these parameters (Fig. 3*B–E*). As anticipated, intra-PVN FGF1 microinjection robustly induced pERK1/2 in the PVN, but not in the ARC-ME (Fig. 3*F*), confirming that FGF1 signaling was limited to the former area.

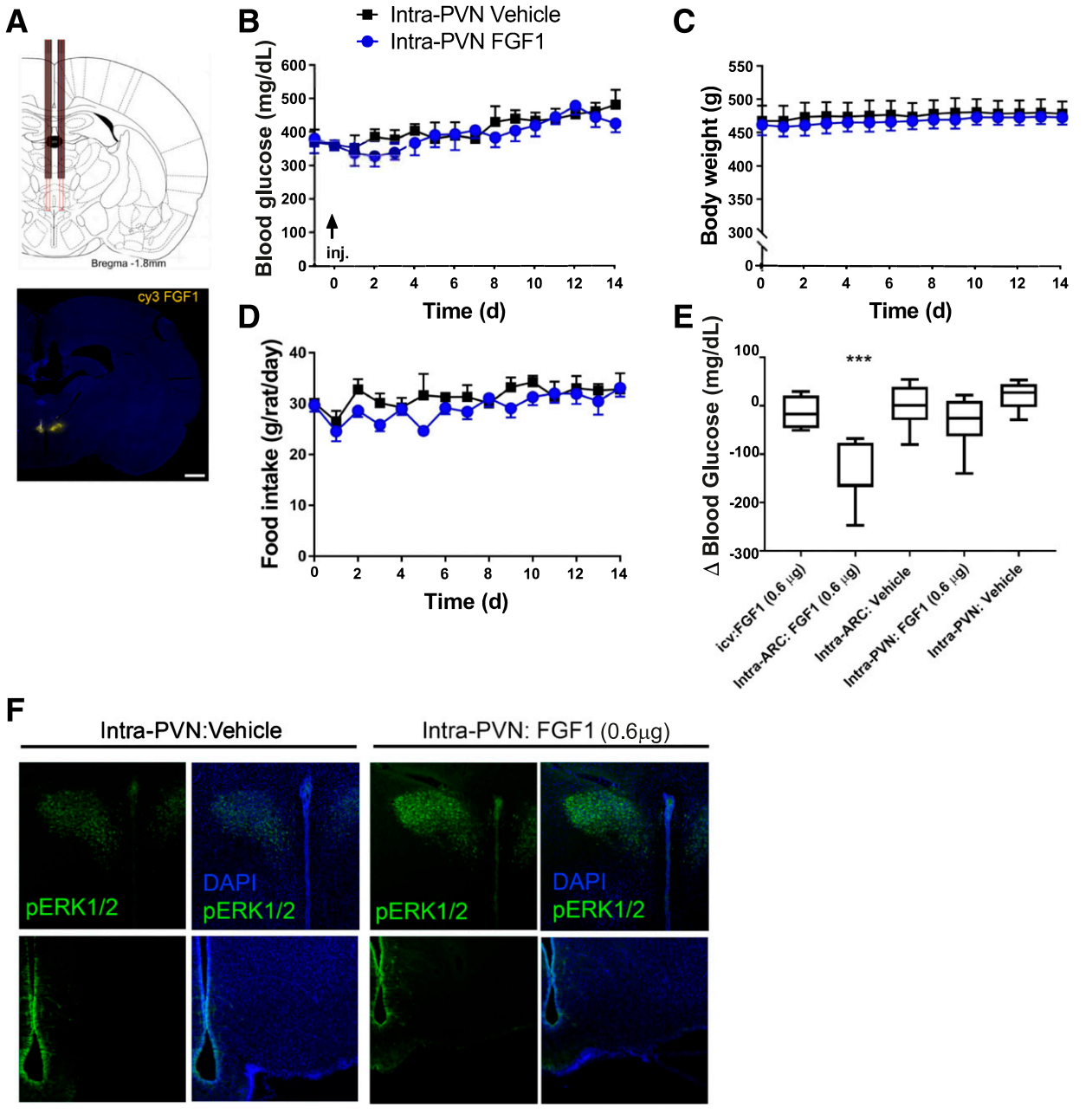

Figure 3—Effect of intra-PVN FGF1 microinjection on blood glucose levels in ZDF rats. *A*: Scale diagram of bilateral intra-PVN guide cannula placement (top panel) and representative image of Cy3 FGF1 injectate spread following intra-PVN microinjection (bottom panel). Scale bar: 1,000 μm. Daily levels of blood glucose (*B*), body weight (*C*), and food intake (*D*) of ZDF rats after a single bilateral microinjection into the PVN of either vehicle (n = 5) or FGF1 (0.3 μg/side, for a total of 0.6 μg; n = 6). No significant differences in group mean values of any of these parameters were observed. Significance determined by linear mixed-model analysis. *E*: Change of blood glucose levels measured 48 h after icv, intra-ARC, or intra-PVN injection of either vehicle or FGF1 in the same animals. ***$P < 0.05$ vs. the other four groups by one-way ANOVA with Tukey post hoc test. *F*: Confocal images of pERK1/2 and DAPI immunostaining in coronal sections collected 20 min after an intra-PVN microinjection of either vehicle or FGF1 (0.3 μg/side; n = 3/group) at the level of either the PVN (top panel) or ARC-ME (bottom panel) in Wistar rats. Data are mean ± SEM. d, days.

DISCUSSION

Based on activation of MAPK/ERK downstream of FGF receptors (measured by pERK1/2 immunostaining), we report that the hypothalamic ARC-ME and PVN are the principal brain areas acutely engaged by FGF1 after icv administration. We further demonstrate that in the ZDF rat model of T2D, the effect of icv FGF1 to normalize diabetic hyperglycemia in a sustained manner is recapitulated by local delivery of FGF1 to the ARC-ME, but not to the PVN. Since the dose of FGF1 used for microinjection in these studies was below the threshold for inducing detectable glucose lowering when given icv, the effects cannot be attributed to leakage into the cerebrospinal fluid and subsequent action elsewhere in the brain. Together, these findings identify the ARC-ME area as a target for the sustained antidiabetic action of FGF1 in the brain.

As a first step toward understanding the cellular basis for this FGF1 response, we colocalized FGF1-induced pERK1/2 with markers of tanycytes (vimentin), astrocytes (GFAP), and neurons (NeuN) in the ARC-ME. Interestingly, whereas a cellular response to FGF1 was readily detected in tanycytes and astrocytes, pERK1/2 induction was not observed in neurons. Although we cannot rule out the possibility that alternative intracellular signaling pathways were activated in neurons, these findings support a model in which effects of FGF1 on ARC-ME neurocircuit activity occur indirectly as a consequence of actions on glial cells rather than via a direct effect on neurons. This notion is consistent with evidence implicating both tanycytes and astrocytes in brain glucose sensing (16–18) and with the known role played by astrocytes to regulate neuronal function (19). Future investigation is warranted into the role of glial cells as mediators of the neuronal response to FGF1.

In light of growing evidence of a key role for ARC-ME neurocircuits in the regulation of glucose homeostasis (20–22), our finding that sustained glucose lowering can be induced by FGF1 action limited to this brain area is not completely unexpected. As a circumventricular organ, the ME is characterized by the absence of a blood–brain barrier, thereby providing glia and neurons in the medial aspect of the ARC with access to circulating nutrients and hormones crucial to metabolic homeostasis. The ARC-ME has also been linked to the pathogenesis of obesity and T2D by virtue of the reactive gliosis involving activation of microglia and astrocytes that develops in this area during high-fat diet feeding (23). Indeed, recent evidence suggests that this gliosis is both necessary and sufficient for obesity to develop on this diet (24). Future studies are warranted to determine how FGF1 action on glial cells in this brain area affects circuits involved in the control of energy balance as well as glucose homeostasis.

Although our data highlight the role of the ARC-ME in the sustained remission of diabetic hyperglycemia induced by FGF1, we cannot exclude contributions made by any brain area other than the PVN. Another potential limitation pertains to our decision to map FGF1-responsive brain areas in normal rats, while performing the microinjection studies in diabetic ZDF rats, as it is conceivable that the response differs between these two rat strains. Offsetting this concern is the need to establish the pattern of brain FGF1 responsiveness in normal animals and then using this information to guide our work, as we have done. Future studies are warranted to investigate whether and how obesity and diabetes might affect brain responsiveness to FGF1. Last, our work also does not address whether an action of FGF1 in the ARC-ME is necessary as well as sufficient to explain this effect. Ongoing studies seek to answer these questions and to clarify the cellular and molecular mechanisms involved in the sustained remission of diabetes induced by the central action of FGF1.

Acknowledgments. The authors thank Nathanial Peters at the University of Washington Keck Imaging Center for technical assistance and the National Institutes of Health (S10-OD-016240) for support to the W.M. Keck Foundation Center for Advanced Studies in Neural Signaling. The authors also thank Bao Phan, University of Washington, for technical support and Dr. Zaman Mirzadeh, Barrow Neurological Institute, as well as members of the Thaler and Schwartz laboratories, University of Washington, for many meaningful discussions.

Funding. This work was supported by National Institute of Diabetes and Digestive and Kidney Diseases grants DK-114474 (to J.M.S.), DK-101997 (to M.W.S.), DK-089056 (to G.J.M.), DK-083042 (to G.J.M. and M.W.S.), and DK-035816 (to G.J.M. and M.W.S.) and Nutrition Obesity Research Center grant DK-035816 (to G.J.M. and M.W.S.) at the University of Washington. J.M.B. is supported by National Heart, Lung, and Blood Institute T32 training grant HL-007312 and the Diabetes Research Center Samuel and Althea Stroum Endowed Graduate Fellowship.

Duality of Interest. Funding in support of these studies was provided to M.W.S. by Novo Nordisk A/S (CMS-431104). No other potential conflicts of interest relevant to this article were reported.

Author Contributions. J.M.B. contributed to the experimental design, researched data, contributed to data analysis and discussion, and wrote the manuscript. J.M.S. and M.W.S. contributed to the experimental design, researched data, contributed to the discussion, and reviewed and edited the manuscript. M.E.M. and H.T.N. assisted with experimental procedures. A.S., R.J., and G.J.M. contributed to the discussion and reviewed and edited the manuscript. All authors approved the final version of this manuscript. M.W.S. is the guarantor of this work and, as such, had full access to all of the data in the study and takes responsibility for the integrity of the data and the accuracy of the data analysis.

Data Availability. The data sets generated during and/or analyzed during the current study are available from the corresponding author on reasonable request.

Prior Presentation. Parts of this study were presented at the 78th Scientific Sessions of the American Diabetes Association, Orlando, FL, 22–26 June 2018, and the American Society for Biochemistry and Molecular Biology Deuel Conference, Coronado, CA, 6–9 March 2018.

References

1. Morton GJ, Matsen ME, Bracy DP, et al. FGF19 action in the brain induces insulin-independent glucose lowering. J Clin Invest 2013;123:4799–4808

2. Sarruf DA, Thaler JP, Morton GJ, et al. Fibroblast growth factor 21 action in the brain increases energy expenditure and insulin sensitivity in obese rats. Diabetes 2010;59:1817–1824

3. Scarlett JM, Rojas JM, Matsen ME, et al. Central injection of fibroblast growth factor 1 induces sustained remission of diabetic hyperglycemia in rodents. Nat Med 2016;22:800–806

4. Lan T, Morgan DA, Rahmouni K, et al. FGF19, FGF21, and an FGFR1/β-klotho-activating antibody act on the nervous system to regulate body weight and glycemia. Cell Metab 2017;26:709–718.e3

5. Scarlett JM, Muta K, Brown JM, et al. Peripheral mechanisms mediating the sustained antidiabetic action of FGF1 in the brain. Diabetes 2019;68:654–664

6. Choubey L, Collette JC, Smith KM. Quantitative assessment of fibroblast growth factor receptor 1 expression in neurons and glia. PeerJ 2017;5: e3173

7. Belluardo N, Wu G, Mudo G, Hansson AC, Pettersson R, Fuxe K. Comparative localization of fibroblast growth factor receptor-1, -2, and -3 mRNAs in the rat brain: in situ hybridization analysis. J Comp Neurol 1997;379:226–246

8. Roh E, Song DK, Kim MS. Emerging role of the brain in the homeostatic regulation of energy and glucose metabolism. Exp Mol Med 2016;48:e216

9. Etgen GJ, Oldham BA. Profiling of Zucker diabetic fatty rats in their progression to the overt diabetic state. Metabolism 2000;49:684–688

10. Zakrzewska M, Haugsten EM, Nadratowska-Wesolowska B, et al. ERK-mediated phosphorylation of fibroblast growth factor receptor 1 on Ser777 inhibits signaling. Sci Signal 2013;6:ra11

11. Wu AL, Kolumam G, Stawicki S, et al. Amelioration of type 2 diabetes by antibody-mediated activation of fibroblast growth factor receptor 1. Sci Transl Med 2011;3:113ra126

12. R Development Core Team. *R: A Language and Environment for Statistical Computing*. Vienna, Austria, R Foundation for Statistical Computing, 2013

13. RStudio Team. *RStudio: Integrated Development Environment for R*. 1.1.419 ed. Boston, MA, RStudio, 2016

14. Pinheiro J, Bates D, DebRoy S, Sarkar D; R Core Team. nlme: Linear and Nonlinear Mixed Effects Models [Internet], 2013. Available from https://cran.r-project.org/package=nlme. Accessed 4 January 2019

15. Noguchi K, Gel YR, Brunner E, Konietschke F. nparLD: An R software package for the nonparametric analysis of longitudinal data in factorial experiments. J Stat Softw 2012;50:1–23

16. Benford H, Bolborea M, Pollatzek E, et al. A sweet taste receptor-dependent mechanism of glucosensing in hypothalamic tanycytes. Glia 2017;65: 773–789

17. Elizondo-Vega R, Cortes-Campos C, Barahona MJ, Oyarce KA, Carril CA, García-Robles MA. The role of tanycytes in hypothalamic glucosensing. J Cell Mol Med 2015;19:1471–1482

18. Rogers RC, McDougal DH, Ritter S, Qualls-Creekmore E, Hermann GE. Response of catecholaminergic neurons in the mouse hindbrain to glucoprivic stimuli is astrocyte dependent. Am J Physiol Regul Integr Comp Physiol 2018;315: R153–R164

19. Covelo A, Araque A. Neuronal activity determines distinct gliotransmitter release from a single astrocyte. eLife 2018;7:e32237

20. Bentsen MA, Mirzadeh Z, Schwartz MW. Revisiting how the brain senses glucose—and why. Cell Metab 2019;29:11–17

21. Deem JD, Muta K, Scarlett JM, Morton GJ, Schwartz MW. How should we think about the role of the brain in glucose homeostasis and diabetes? Diabetes 2017;66:1758–1765

22. Meek TH, Nelson JT, Matsen ME, et al. Functional identification of a neurocircuit regulating blood glucose. Proc Natl Acad Sci U S A 2016;113:E2073–E2082

23. Thaler JP, Yi CX, Schur EA, et al. Obesity is associated with hypothalamic injury in rodents and humans. J Clin Invest 2012;122:153–162

24. Valdearcos M, Douglass JD, Robblee MM, et al. Microglial inflammatory signaling orchestrates the hypothalamic immune response to dietary excess and mediates obesity susceptibility. Cell Metab 2018;27:1356